J. Opt. **14** (2012) 015701 (8pp) doi:10.1088/2040-8978/14/1/015701

Diffraction of ultrashort Gaussian pulses within the framework of boundary diffraction wave theory

Peeter Piksarv[1], Pamela Bowlan[2], Madis Lõhmus[1], Heli Valtna-Lukner[1], Rick Trebino[2] and Peeter Saari[1,3]

[1] Institute of Physics, University of Tartu, Riia 142, Tartu 51014, Estonia
[2] School of Physics, Georgia Institute of Technology, 837 State Street NW, Atlanta, GA 30332, USA
[3] Estonian Academy of Sciences, Kohtu 6, Tallinn 10130, Estonia

E-mail: peeter.piksarv@ut.ee

Received 20 October 2011, accepted for publication 16 November 2011
Published 8 December 2011
Online at stacks.iop.org/JOpt/14/015701

Abstract
We study the diffraction of Gaussian pulses and beams within the framework of boundary diffraction wave theory. For the first time the boundary diffraction wave theory is applied to pulsed Gaussian beams, and it is shown that the diffracted field of a pulsed Gaussian beam on a circularly symmetric aperture can be evaluated by a single 1D integration along the diffracting aperture at every point of interest. We compare theoretical simulations to experimental measurements of ultrashort pulses diffracted off a circular aperture, an opaque disc, an annular aperture, and a system of four concentric annular apertures. Using the recently developed SEA TADPOLE measurement technique, we obtain micron spatial and femtosecond temporal resolutions in the spatio-temporal measurements of the diffracted fields.

Keywords: diffraction theory, ultrafast measurements, boundary diffraction wave

(Some figures may appear in colour only in the online journal)

1. Introduction

Spatio-temporal couplings of ultrashort pulses have come to play ever increasing—both desirable and undesirable—roles in important applications, including pulse compression, shaping, imaging, and focusing (see e.g. [1–3] and references therein). The propagation of an ultrashort pulse exposes it to many such distortions, of which some remain rather surprising. For example, even a simple circular aperture creates a trailing pulse that, in the case of femtosecond laser pulses, is quite distinguishable from the main pulse [4–9]. As a result, detailed investigation of ultrashort pulse propagation and focusing is also of fundamental interest in fields that require focusing them, including nonlinear optics, lithography, micro-machinery, biology, and medicine.

It turns out to be surprisingly enlightening to study the diffraction of ultrashort pulses. Although somewhat forgotten, the boundary diffraction wave (BDW) theory works well for intuitively explaining the complex spatio-temporal effects for ultrashort pulse propagation [4, 6]. The BDW theory, which has been shown to be mathematically equivalent to the Fresnel–Kirchhoff diffraction theory by Miyamoto and Wolf [10, 11], provides an elegant alternative approach to wave propagation. Though the theory was first developed for plane and spherical waves, it has been shown by Otis [12, 13] that BDW theory is also applicable to Gaussian beams within the limits of the paraxial approximation. The benefits of expressing the diffracted wave as a sum of the so-called geometric wave and boundary wave become especially obvious when considering ultrashort pulses, for which the two waves often separate in time and space and so can be more readily identified—provided that a suitable measurement technique of such exotic events is available.

Fortunately, direct measurements of the spatio-temporal electric field $E(x, y, z, t)$ of arbitrary ultrashort pulses have recently become possible using a technique based on spectral interferometry called SEA TADPOLE [14–17]. It records 'snapshots in flight' or spatio-temporal slices of the field

amplitude and phase with μm spatial and fs temporal resolutions. For a detailed description of the method, see for example [15, 18].

In the present paper, we will develop the expression for the boundary wave for a diffracted Gaussian pulse in the case of a circularly symmetric aperture. In section 3 the simulation results are compared with the SEA TADPOLE measurements of the diffracted Gaussian pulses in the case of a circular aperture, an opaque disc, an annular aperture and a system of four concentric annular apertures as a diffracting obstacle.

2. The boundary wave for a Gaussian pulse

The Gaussian beam is a well-known solution of the paraxial wave equation. The field of a monochromatic Gaussian beam with angular frequency ω can be written as [19]

$$U(\rho, z, \omega) = \frac{q(0)}{q(z)} \mathrm{e}^{\mathrm{i}k\frac{\rho^2}{2q(z)}} \mathrm{e}^{\mathrm{i}kz} H(\omega), \tag{1}$$

where $q(z) = z + d - \mathrm{i}z_\mathrm{R}$ is the complex beam parameter and $z_\mathrm{R} = kw_0^2/2$ is the Rayleigh diffraction length, with $z = -d$ as the location of the waist of a smallest spot size w_0. $H(\omega)$ is a frequency-dependent parameter and $k = 2\pi/\lambda$ is the wavenumber, where λ denotes the wavelength.

If the diffracting aperture is located at $z = 0$, then according to the BDW theory the diffracted wave at a point $P = (\rho, \varphi, z)$ in the region $z > 0$ behind the aperture can be represented as [11]

$$U_\mathrm{D}(P, \omega) = U_\mathrm{B}(P, \omega) + U_\mathrm{G}(P, \omega). \tag{2}$$

Here U_G is a wave that propagates according to the laws of geometrical optics and is equal to the incident wave in the points of direct beam and is zero elsewhere. U_B is called the boundary wave and it can be expressed by a line integral along the edge of diffracting aperture Γ as

$$U_\mathrm{B}(P, \omega) = \oint_\Gamma \boldsymbol{W}(P, Q)\, \mathrm{d}\boldsymbol{l}, \tag{3}$$

where $\boldsymbol{W}$ is a vector potential associated with the incident field, $\boldsymbol{l}$ is the element vector of Γ, and Q represents a typical point in the aperture. Otis [12, 13] has shown that within the paraxial approximation the vector potential $\boldsymbol{W}$ for a Gaussian beam $U(Q)$ can be expressed as

$$\boldsymbol{W}(P, Q) = U(Q) \frac{\mathrm{e}^{\mathrm{i}ks}}{4\pi s} \frac{\hat{\boldsymbol{s}} \times \boldsymbol{p}}{1 + \hat{\boldsymbol{s}} \cdot \boldsymbol{p}}, \tag{4}$$

where s denotes the distance PQ and $\hat{\boldsymbol{s}}$ the corresponding unit vector. The vector $\boldsymbol{p}$ represents the gradient of the phase of the incident wave at Q i.e. $\boldsymbol{p} = \nabla_Q[z + \rho^2/2q(z)]$.

If the Gaussian beam is normally incident on a circular aperture with a radius a, then the geometric wave is given by [12, 20]

$$U_\mathrm{G}(P, \omega) = \begin{cases} U(P, \omega) & \text{for } \rho < \rho_\mathrm{h}(z), \\ 0 & \text{for } \rho > \rho_\mathrm{h}(z), \end{cases} \tag{5}$$

where

$$\rho_\mathrm{h} = a|q(z)/q(0)| \tag{6}$$

is the shadow boundary. For the boundary wave the following expression may be obtained [20]:

$$U_\mathrm{B}(P, \omega) = U(Q, \omega) \frac{a}{4\pi} \int_0^{2\pi} \mathrm{e}^{\mathrm{i}ks(\psi)} f(\psi)\, \mathrm{d}\psi, \tag{7}$$

where

$$f(\psi) = \frac{\rho[1 - \frac{a^2}{2q^2(0)}] \cos\psi - a[1 - \frac{a^2}{2q^2(0)}] - \frac{az}{q(0)}}{s(\psi)[s(\psi) - \frac{a\rho}{q(0)} \cos\psi + \frac{a^2}{q(0)} - z(1 - \frac{a^2}{2q^2(0)})]}, \tag{8}$$

and

$$s(\psi) = \sqrt{z^2 + a^2 + \rho^2 - 2a\rho\cos\psi}. \tag{9}$$

A Gaussian pulse can be written as

$$u(\rho, z, t) = \frac{q(0)}{q(z)} v\left(t - \frac{z}{c} - \frac{\rho^2}{2cq(z)}\right) \mathrm{e}^{-\mathrm{i}k_0 c(t - \frac{z}{c} - \frac{\rho^2}{2cq(z)})}, \tag{10}$$

where

$$v(t) = \exp\left(-4 \ln 2 \frac{t^2}{\tau^2}\right) \tag{11}$$

is the temporal envelope of the pulse and τ the pulse duration (FWHM of field strength). In order to develop an equation for a diffracted Gaussian pulse a similar approach to [4] can be taken, where the BDW theory was developed for plane and spherical wave pulses. Next an equation for a boundary wave for a diffracted Gaussian pulse is developed.

The polychromatic field can be expressed as a superposition of monochromatic waves

$$u(P, t) = \mathcal{F}^{-1}\{U(P, \omega)\}, \tag{12}$$

where $\mathcal{F}^{-1}$ denotes the inverse Fourier transform. For an isodiffracting pulse defined by condition $z_\mathrm{R} = \mathrm{const}$ [21], the Gaussian pulse as written in (10) can be obtained from equation (1) by using the spectrum

$$H(\omega) = \frac{\tau}{4\sqrt{\pi \ln 2}} \mathrm{e}^{-\frac{\tau^2}{16 \ln 2}(\omega_0 - \omega)^2}, \tag{13}$$

where $\omega_0 = k_0 c$ is the central frequency. According to the linear properties of the Fourier transform, it is possible to decompose the incident beam to its monochromatic components and the field of a diffracted pulse can be written similarly to (2):

$$u_\mathrm{D}(P, t) = u_\mathrm{G}(P, t) + u_\mathrm{B}(P, t), \tag{14}$$

where

$$u_\mathrm{G}(P, t) = \mathcal{F}^{-1}\{U_\mathrm{G}(P, \omega)\}, \tag{15}$$

$$u_\mathrm{B}(P, t) = \mathcal{F}^{-1}\{U_\mathrm{B}(P, \omega)\}. \tag{16}$$

The $U_\mathrm{G}(P, \omega)$ and $U_\mathrm{B}(P, \omega)$ are given correspondingly by equations (5) and (7). $u_\mathrm{B}(P, t)$ and $u_\mathrm{G}(P, t)$ are the main and boundary wave pulses [4].

The field of the pulse propagating according to the laws of geometrical optics is straightforwardly determined from

equation (5) as

$$u_{\mathrm{G}}(P,t)=\begin{cases}u(P,t) & \text{for } \rho<\rho_{\mathrm{h}}(z),\\ 0 & \text{otherwise,}\end{cases} \tag{17}$$

where the shadow boundary is defined by (6). The boundary wave pulse can be obtained from the inverse Fourier transform of equation (7) and can be written as

$$u_{\mathrm{B}}(P,t)=\frac{a}{4\pi}\mathrm{e}^{-\mathrm{i}k_0(ct-\frac{a^2}{2q(0)})}\times\int_0^{2\pi}v\left(t-\frac{a^2}{2cq(0)}-\frac{s(\psi)}{c}\right)\mathrm{e}^{\mathrm{i}k_0 s(\psi)}f(\psi)\,\mathrm{d}\psi, \tag{18}$$

where the functions $f(\psi)$ and $s(\psi)$ are given by equations (8) and (9), respectively, and the temporal envelope $v(t)$ by (11). Equation (18) can be numerically integrated using an adaptive quadrature method.

It should be noted that on the optical axis the integrand in the equation of the boundary wave pulse is independent of the angle ψ and an analytic expression for the electric field can be derived

$$u_{\mathrm{B0}}(z,t)=-\frac{a^2}{2s_0(z)}\frac{q(z)}{q(0)}\times\frac{1-\frac{z}{q(0)}+\frac{a^2}{2q^2(0)}}{s_0(z)+\frac{a^2}{q(0)}-z(1-\frac{a^2}{2q^2(0)})}u(0,z,t-T(z)), \tag{19}$$

where $s_0(z)=\sqrt{a^2+z^2}$ and

$$T(z)=\frac{s_0(z)}{c}+\frac{a^2}{2cq(0)}-\frac{z}{c} \tag{20}$$

determines the time delay between the main and boundary wave pulse. In the limiting case of plane and spherical waves i.e. $w_0\to\infty$ or $d\to\infty$ respectively, this result is consistent with the on-axis field of the boundary wave pulse given in [4]. In the following, equation (18) was used in the simulations to calculate the field of diffracted pulses.

3. Boundary pulse simulations in comparison with experimental results

At first, an overview of the experimental setup is given with which the BDW simulation parameters were chosen to match. As an ultrashort pulse laser source the KM Labs Ti:sapphire oscillator with ~33 nm of bandwidth and a spot size of 4 mm (FWHM) was used. The central wavelength was $\lambda_0=810$ nm. Complete spatio-temporal measurements of diffracted ultrashort pulses were carried out using a scanning SEA TADPOLE technique [18, 22]. Briefly, it is a variation of spectral interferometry in which a small spatial region of the unknown field is sampled with a single-mode optical fibre and interfered with a known reference pulse in a spectrometer. $E(\lambda)$ can be reconstructed for that spatial point from a measured camera image and scanning the fibre throughout the cross section of the unknown beam yields $E(P,\lambda)$ which can be Fourier transformed to the time domain to retrieve $E(P,t)$. The plots of the measurements can be depicted as

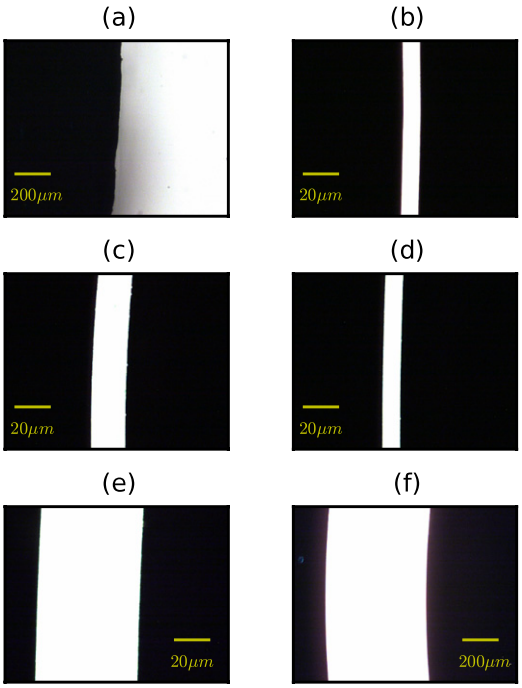

Figure 1. Optical microscope images of the boundaries: (a) the opaque disc; (b) the single annular slit; (c)–(f) the individual slits of the system of four concentric annular slits from innermost to outermost.

'snapshots in flight' or spatio-temporal slices of the amplitude of the electric field of the pulses. As our setup had cylindrical symmetry, the scanning was performed with the fibre only along the x-axis at $y=0$. In order to study the z-dependence of the diffraction pattern, the diffracting aperture was translated away from the fibre.

The diffracted field of ultrashort pulses was measured behind four different obstacles: a circular aperture, an opaque disc, an annular slit and a system of four concentric annular slits. The diameter of the circular aperture was 4.4 mm and it was made of 3.2 mm thick metal. The 4 mm diameter disc was fabricated of aluminum sheet with a thickness of 0.2 mm and was glued onto a thin glass substrate. Annular slits were engraved onto metal-coated glass substrates. The single slit had a diameter of 5.4 mm and a width of 10 μm, the dark region of the single annular slit transmitted 0.63% of the light intensity at the used wavelength. The concentric annular slits had diameters of 2.1, 4.7, 6.3, and 12.5 mm with corresponding slit widths of 20, 10, 60, and 610 μm. During the experiments it was noted that the smoothness of the edge contour of the obstacle was critical for the intensity of the boundary wave pulse. Figure 1 shows the optical microscope images of the edge contours of the obstacles. However, the thickness of the diffracting aperture did not seem to alter the observability of the boundary wave pulse.

Computer simulations were carried out by using equation (14), where the geometric pulse was defined by (17) and the boundary wave pulse was obtained by numerical integration in (18). Numerical integration was carried out by Mathcad. The simulation parameters have been taken closely similar to the experimental setup. The integrand itself is rather

inconvenient for integration as it is constant on the z-axis and becomes quickly oscillating off-axis. An adaptive quadrature method gave the best results in terms of time spent versus accuracy. Simpson's rule, which was used for evaluating diffraction integrands in [23], resulted in less accurate results within the same computational time. In the case of insufficient partitions N, there appeared additional 'boundary waves' as is shown in figure 2. On the other hand, a non-adaptive method might be suitable in the case of a small radial and temporal region of interest and may be easier to implement with high speed vector operations.

3.1. Circular aperture and disc

Diffraction from a circular aperture and a circular disc is a well-known problem that has been thoroughly studied. Usually, however, diffraction is considered only by monochromatic illumination. In the case of femtosecond laser pulses, diffraction is a spatio-temporal effect, which can be understood in terms of the BDW theory. There have been several indirect indications of the temporal characteristics of diffracted ultrashort pulses [5, 24], but not until very recently has the full spatio-temporal nature of diffraction been directly measured [6]. In the present work, complete measurements of the diffracted ultrashort laser pulses are compared to the BDW theory that has been generalized to apply to Gaussian pulses.

The measured spatio-temporal field of a pulse diffracted by a 4.4 mm diameter aperture alongside the corresponding simulations is given in figure 3. The normalized amplitude of the field is indicated by the colour map. As the optical path length is kept constant on the reference arm of the interferometer, the pulse, which would be registered at $t = 0$ fs, would propagate at the speed of light. Hence the superluminal velocity of the boundary wave pulse can be

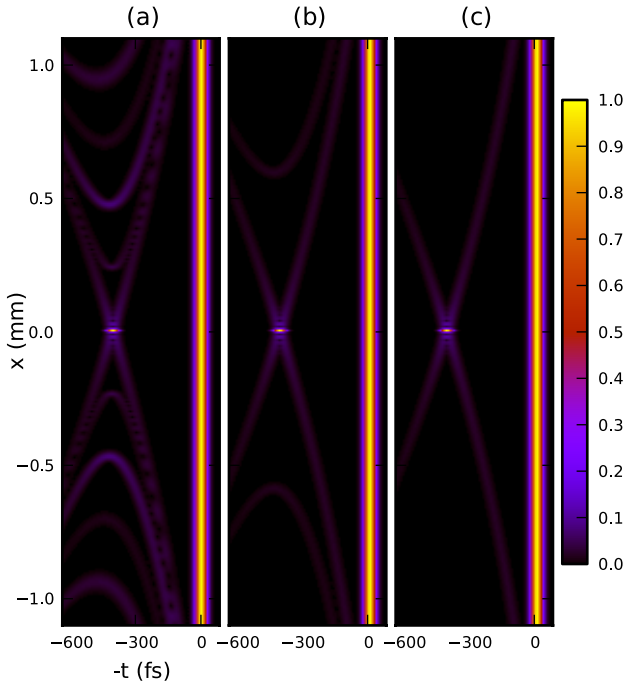

Figure 2. Results of different numerical integration methods for evaluating the boundary wave diffraction integral for a 40 fs plane wave pulse diffracted by a circular aperture 4 mm in diameter 20 mm from the aperture. (a) Simpson's method with $N = 199$ partitions; (b) $N = 499$ partitions respectively; (c) Mathcad's adaptive quadrature method.

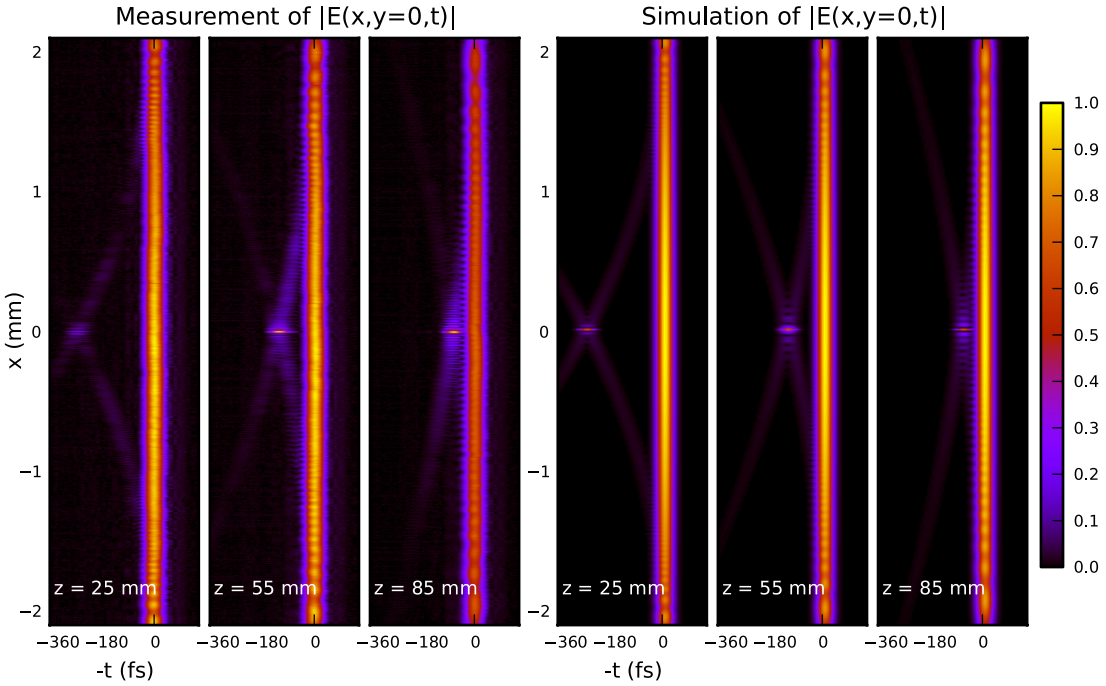

Figure 3. Comparison of the measured and simulated light field amplitudes of an ultrashort pulse diffracted by a circular aperture at three distances behind the aperture.

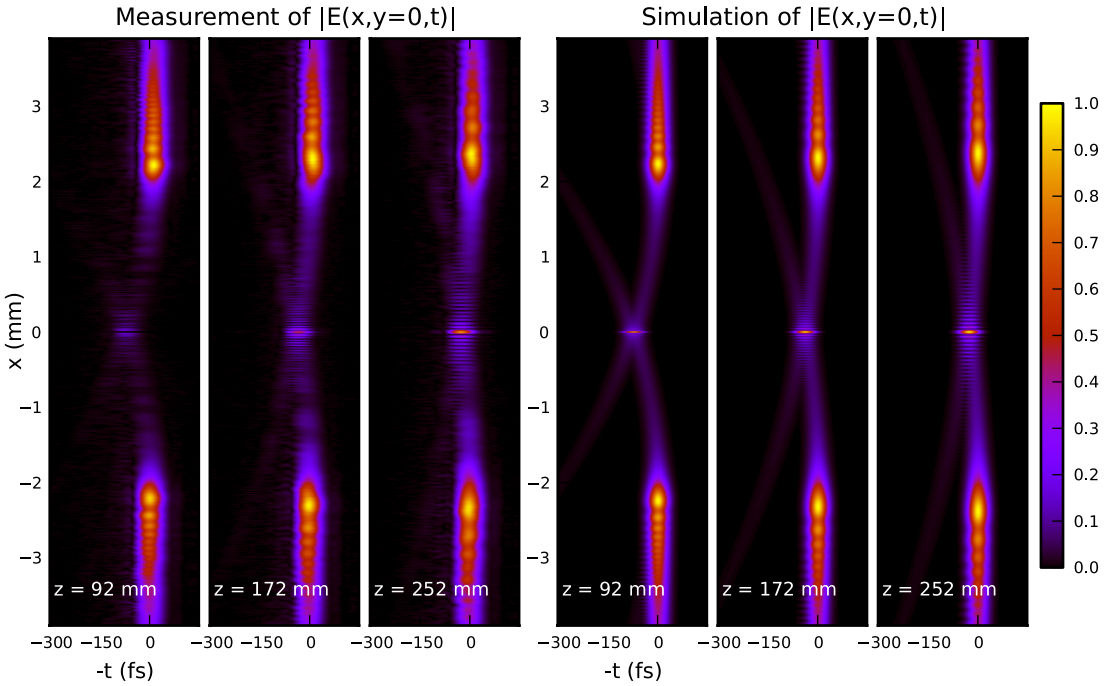

Figure 4. Propagation and evolution of the diffracted pulse behind an opaque disc.

qualitatively determined from the experiment figures as it catches up with the main pulse by increasing the travel distance z. The velocity of the boundary wave pulse on the optical axis decelerates from ∞ at the aperture plane $z = 0$ mm to the speed of light c at $z \to \infty$.

Figure 3 shows good agreement between the BDW theory and the experiment. Variation in the brightness of the main pulse is likely due to the thickness and imperfect surface quality of our aperture. In the temporal profile of the measured impulses there appear ripples before and after the main pulse that are not present in the simulation. This is likely due to the zero-filling before taking the Fourier transform of the measured spectrum. As with the current camera the dark level is tilted, so the elimination of this jump in the measured spectrum is complicated. To some extent the temporal profile of the measured pulses may be affected by the spectral response curve of the camera, but the most important difference originates from the idealization of the pulse spectra to Gaussian not taking into account the real laser spectra. Despite the minor discrepancies, the results show good agreement between the computer simulations and measurements.

The diffraction from an opaque circular disc can be easily derived according to Babinet's principle. The diffracted field can be written as

$$u'_{\mathrm{D}}(P,t) = u'_{\mathrm{G}}(P,t) - u_{\mathrm{B}}(P,t), \tag{21}$$

where

$$u_{\mathrm{G}}(P,t) = \begin{cases} u(P,t) & \text{for } \rho > \rho_{\mathrm{h}}(z), \\ 0 & \text{otherwise,} \end{cases} \tag{22}$$

and $u_{\mathrm{B}}(P,t)$ is given by (18).

The measurements along with the corresponding simulations are shown in figure 4. The similarity with the previously registered diffraction pattern is obvious.

As in the present case the boundary wave pulse and the geometric pulse do not overlap on the optical axis, the measurement of the Arago spot requires a more sensitive measurement device due to the characteristics of the SEA TADPOLE technique. Therefore, the measurements shown in figure 4 are noisier than in the case of a circular aperture. Also, the constructive interference on the optical axis is decreased by any irregularities in the shape of the obstacle and by the serration of the boundary.

The fact that the shadow of an opaque disc starts filling up with light from the centre according to the wave nature of light seems a peculiar effect according to the mainstream diffraction theory or in the case when the diffraction of light is understood literally as bending of the light waves into the shadow region behind an obstacle. On the contrary, according to the BDW theory, the appearance of the Arago spot on the optical axis right behind the obstacle is easily comprehensible.

3.2. Annular slits

Combining the two problems discussed above we look into the diffraction of the fs pulse on an annular slit described by a radius a and slit width of $2\delta a$. Similarly, the diffracted pulse can be expressed by the sum of the geometric pulse and the boundary wave pulse:

$$u_{\mathrm{p}}(P,t) = u''_{\mathrm{G}}(P,t) + u''_{\mathrm{B}}(P,t), \tag{23}$$

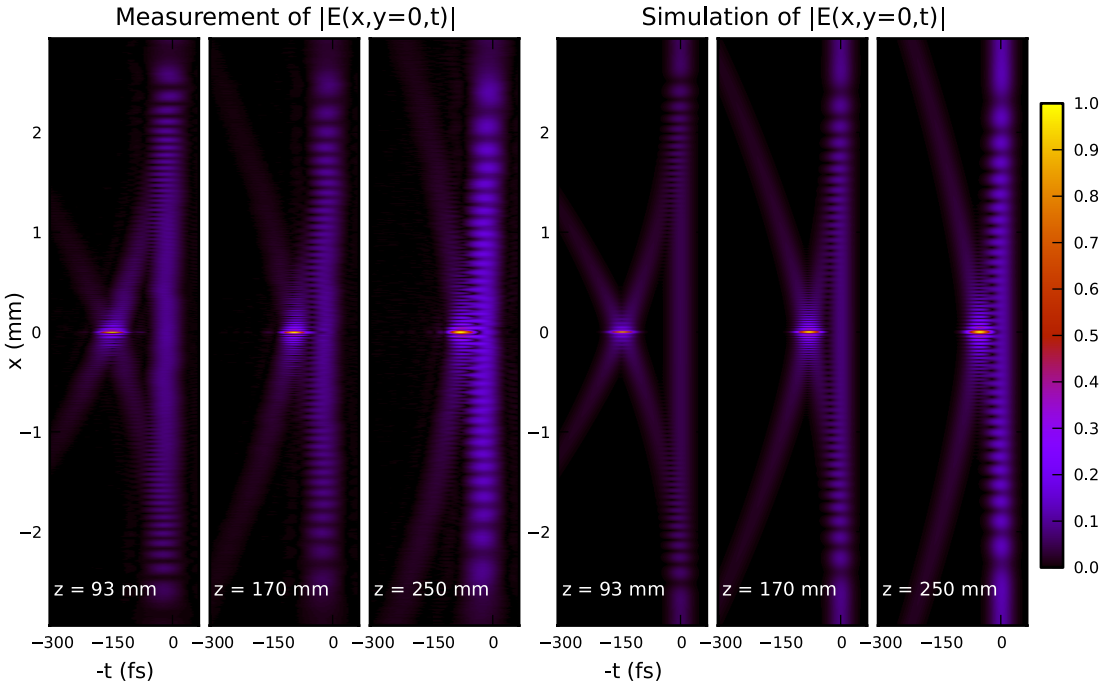

Figure 5. Measured and calculated electric field amplitude of pulse generated behind a thick annular slit on a partially transparent substrate.

where

$$u''_{\mathrm{G}}(P,t) = \begin{cases} u(P,t) & \text{if } \rho > \rho_h(z, a-\delta a) \\ & \text{and } \rho < \rho_{\mathrm{h}}(z, a+\delta a), \\ 0 & \text{otherwise,} \end{cases} \tag{24}$$

The boundary wave pulse for the case of an annular slit can be expressed as a sum of the boundary waves of the inner and outer edge of the slit

$$u''_{\mathrm{B}} = u_{\mathrm{B}}(P,t,a+\delta a) - u_{\mathrm{B}}(P,t,a-\delta a), \tag{25}$$

where $u_{\mathrm{B}}(P,t,a)$ is given by (18) if the radius of the boundary curvature is a. If the width of the annular slit is small enough, then it can be expected that the different boundary wave pulses are not distinguishable in time and space.

Next, the diffracted pulse was measured after the annular slit on a slightly transparent substrate. The measurements with corresponding simulations are shown in figure 5. The partial transmission provided a useful reference pulse, which propagates at the speed of light and should remain at the position $t = 0$ fs even if the optical path lengths on the reference and measurement arms of the interferometer should have somehow changed during the measurement series. Therefore, this series of measurements is a good example of the superluminal characteristics of the boundary wave pulse.

Despite the narrow slit width, the geometric pulse could not be neglected in the simulations, otherwise the diffracted field would be discontinuous in the direct pulse region according to the BDW theory. The slight discrepancy between the measured and the simulated pulses near the optical axis is probably caused by the uncertainty of measured distance z.

Further, the diffracted pulse was measured after a mask which consisted of four concentric annular slits. The results are shown in figure 6. In the first two pictures the boundary waves of the three smallest slits are seen, in the third picture they have caught up with each other and formed one pulse. In the last picture the two trailing pulses correspond to the inner and outer boundary of the largest annular slit. In the first measurement at $z = 22$ mm there appears to be also a weak leading pulse due to the partial transparency of the metallic coating. As it does not appear on other measurements and overlaps in time with smaller boundary pulses further away from the mask, it has not been taken into account in the simulations.

These measurements agree with the spatio-temporal structure shown in [1]. In the present case the number of ring apertures is significantly lower and the individual boundary wave pulses are more separated. Especially in the case of $z =$ 242 mm the measurement resolves the boundary wave pulse of the inner and outer boundary of the largest ring aperture. In figure 6 it is remarkable how refined is the complex spatio-temporal structure of the diffracted pulse resolved by the SEA TADPOLE measurement.

The last results show that more complicated diffraction problems can also be understood by rather simple treatments in the time domain. Even quantitatively, all of the setups discussed in this section are calculated by 1D integration from 0 to π at every point of interest. According to the basis of the BDW theory, the results are equivalent to Fresnel–Kirchhoff's theory and not restricted by Fresnel or Fraunhofer approximations.

4. Conclusions

Employing time-domain characterization of diffraction, the BDW theory aids the general understanding of the diffraction

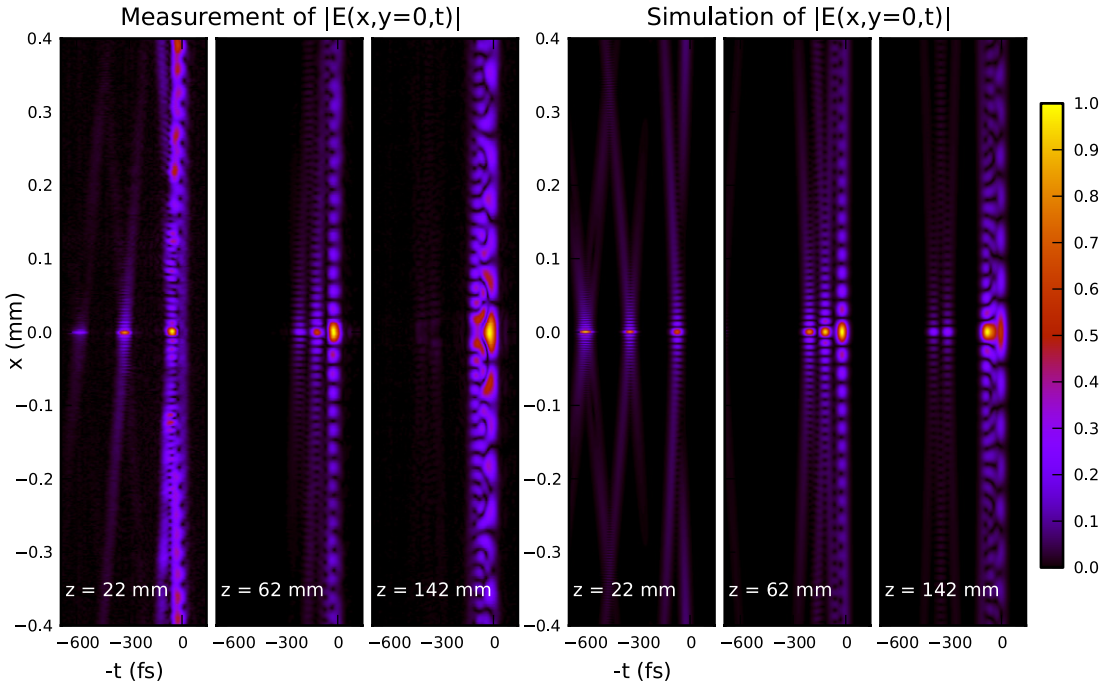

Figure 6. Measured and calculated electric field amplitude of a pulse diffracted by a system of four concentric annular slits of different widths and diameters.

phenomena. It is relatively simple to evaluate qualitatively the propagation of ultrashort pulses by expressing the diffracted wave field as the sum of the boundary and geometric waves. The BDW theory can be applied to Gaussian pulses, and the diffracted field can be evaluated by a simple 1D integration for every point of interest. The experimentally simple and high-spectral resolution variant of spectral interferometry SEA TADPOLE is an excellent method for the characterization of ultrashort pulsed wave fields that are complex in both space and frequency (time).

Acknowledgments

P Saari, H Valtna-Lukner, M Lõhmus, and P Piksarv were supported by the Estonian Science Foundation grant 7870. R Trebino and P Bowlan have been supported by NSF fellowship IGERT-0221600, NSF SBIR grant 053-9595. P Piksarv has been partially supported by graduate school 'Functional materials and processes' receiving funding from the European Social Fund under project 1.2.0401.09-0079 in Estonia.

References

[1] Mendoza-Yero O, Alonso B, Varela O, Mínguez-Vega G, Juan Sola Í, Lancis J, Climent V and Roso L 2010 Spatio-temporal characterization of ultrashort pulses diffracted by circularly symmetric hard-edge apertures: theory and experiment *Opt. Express* **18** 20900–11

[2] Akturk S, Gu X, Bowlan P and Trebino R 2010 Spatio-temporal couplings in ultrashort laser pulses *J. Opt.* **12** 093001

[3] Han P 2008 Spectrum compression of Gaussian pulse from annular aperture in far-field *Japan. J. Appl. Phys.* **47** 914–7

[4] Horváth Z L and Bor Zs 2001 Diffraction of short pulses with boundary diffraction wave theory *Phys. Rev.* E **63** 026601

[5] Horváth Z L, Klebniczki J, Kurdi G and Kovács A 2004 Experimental investigation of the boundary wave pulse *Opt. Commun.* **239** 243–50

[6] Saari P, Bowlan P, Valtna-Lukner H, Lõhmus M, Piksarv P and Trebino R 2010 Basic diffraction phenomena in time domain *Opt. Express* **18** 11083–8

[7] Lõhmus M, Bowlan P, Trebino R, Valtna-Lukner H, Piksarv P and Saari P 2010 Directly recording diffraction phenomena in the time domain *Lithuanian J. Phys.* **50** 69–74

[8] Saari P, Bowlan P, Valtna-Lukner H, Lõhmus M, Piksarv P and Trebino R 2010 Time-and-space-domain study of diffracting and non-diffracting light pulses *Lithuanian J. Phys.* **50** 121–7

[9] Saari P, Bowlan P, Valtna-Lukner H, Lõhmus M, Piksarv P and Trebino R 2010 Directly recording diffraction phenomena in time domain *Laser Phys.* **20** 948–53

[10] Miyamoto K and Wolf E 1962 Generalization of the Maggi–Rubinowicz theory of the boundary diffraction wave—Part I *J. Opt. Soc. Am.* **52** 615–22

[11] Miyamoto K and Wolf E 1962 Generalization of the Maggi–Rubinowicz theory of the boundary diffraction wave—Part II *J. Opt. Soc. Am.* **52** 626–36

[12] Otis G 1974 Application of the boundary-diffraction-wave theory to Gaussian beams *J. Opt. Soc. Am.* **64** 1545–50

[13] Otis G, Lachambre J-L, Lit J W Y and Lavigne P 1977 Diffracted waves in the shadow boundary region *J. Opt. Soc. Am.* **67** 551–3

[14] Bowlan P, Gabolde P, Shreenath A, McGresham K, Trebino R and Akturk S 2006 Crossed-beam spectral interferometry: a simple, high-spectral-resolution method for completely characterizing complex ultrashort pulses in real time *Opt. Express* **14** 11892–900

[15] Bowlan P, Gabolde P, Coughlan M A, Trebino R and Levis R J 2008 Measuring the spatiotemporal electric field of ultrashort pulses with high spatial and spectral resolution *J. Opt. Soc. Am.* B **25** A81–92
[16] Bowlan P, Valtna-Lukner H, Lõhmus M, Piksarv P, Saari P and Trebino R 2009 Measuring the spatiotemporal field of ultrashort bessel-x pulses *Opt. Lett.* **34** 2276–8
[17] Valtna-Lukner H, Bowlan P, Lõhmus M, Piksarv P, Trebino R and Saari P 2009 Direct spatiotemporal measurements of accelerating ultrashort bessel-type light bullets *Opt. Express* **17** 14948–55
[18] Bowlan P, Gabolde P and Trebino R 2007 Directly measuring the spatio-temporal electric field of focusing ultrashort pulses *Opt. Express* **15** 10219–30
[19] Deschamps G A 1971 Gaussian beam as a bundle of complex rays *Electron. Lett.* **7** 684–5
[20] Takenaka T, Kakeya M and Fukumitsu O 1980 Asymptotic representation of the boundary diffraction wave for a Gaussian beam incident on a circular aperture *J. Opt. Soc. Am.* **70** 1323–8
[21] Heyman E and Melamed T 1994 Certain considerations in aperture synthesis of ultrawideband/short-pulse radiation *IEEE Trans. Antennas Propag.* **42** 518–25
[22] Bowlan P, Fuchs U, Trebino R and Zeitner U D 2008 Measuring the spatiotemporal electric field of tightly focused ultrashort pulses with sub-micron spatial resolution *Opt. Express* **16** 13663–75
[23] Cooper I J, Sheppard C J R and Sharma M 2002 Numerical integration of diffraction integrals for a circular aperture *Optik* **113** 293–8
[24] Chauvat D, Emile O, Brunel M and Floch A Le 2002 Direct measurement of the central fringe velocity in Young-type experiments *Phys. Lett.* A **295** 78–80